Molecular Passivation of Mercury−Silicon (p-type) Diode Junctions: Alkylation, Oxidation, and Alkylsilation

Yong-Jun Liu and Hua-Zhong Yu*

Department of Chemistry, Simon Fraser University, Burnaby, British Columbia V5A 1S6, Canada

Received: March 28, 2003; In Final Form: May 23, 2003

To evaluate the electrical performance of molecularly modified metal−semiconductor diode junctions, organic monolayers were grafted on both hydrogen-terminated and oxidized silicon (p-type) surfaces. Three model systems, i.e., $Hg|C_{12}H_{25}-Si$, $Hg|SiO_2-Si$, and $Hg|C_{12}H_{25}SiO_3-SiO_2-Si$, were prepared and systematically characterized based on their current−voltage and capacitance−voltage properties. The experimental results showed that mercury−silicon junctions modified with *n*-dodecyl monolayer display better rectifying behavior, i.e., larger rectifying ratio and smaller empirical ideality factor (i.e., close to unity), than those passivated with SiO_2 thin films and *n*-dodecylsiloxane monolayers (formed on oxidized silicon). The differential capacitance measurements revealed that organic modified junctions (both alkylated and alkylsilated samples) have substantially lower densities of interface states in comparison with that of $Hg|SiO_2-Si$. This work provides a clear assessment of the varied device performance among differently prepared metal−molecule−semiconductor junctions, which is complementary to the topic studies on the electron transport across these molecular interfaces. More importantly, the present research augments the potential applications of molecular modification and surface engineering in the fabrication of silicon-based microelectronic devices.

1. Introduction

Metal−semiconductor (M−S) junctions represent the essential and basic building blocks of microelectronic devices and have been commonly used in creating important circuit elements including ohmic contacts, Schottky diodes, and metal−semiconductor field-effect transistors (MSFET).[1] Upon the introduction of organic modification to semiconductor materials, research has been very active with an ultimate goal to molecularly manipulate the formation, operation, and tunability of *metal−molecule−semiconductor* devices.[2] Junctions prepared from various metal contacts on different silicon surfaces have been extensively studied for many years,[3−10] simply because of the critical importance of silicon in modern semiconductor technology.

Silicon is relatively inert chemically at room temperature. However, clean silicon surfaces are unavoidably contaminated and thermally oxidized between different processing steps upon exposure to air, chemicals, process gases, or even vacuum.[11] Silicon oxide (SiO_2) is so stable that silicon wafers that leave vendor sites are normally protected by very thin oxide films (less than 20 Å, i.e., a few atomic layers). These protective layers were obtained by one-step chemical oxidation in RCA or Piranha solutions.[12] In today's semiconductor industry, silicon oxide films are extremely useful in electronically passivating bulk silicon and insulating electrical interconnects and active devices, yet they are facing fundamental physical limits of miniaturization (i.e., the breakdown of the electronic performance once the thickness reaches the nanometer range).[13] In fact, metal junctions formed on oxidized silicon surfaces have been extensively studied since the 1970s,[3] in contrast to the relatively recent investigations of those formed on hydrogen-terminated silicon surfaces (H−Si).[4] The pioneering research on diode junctions formed from both hydrogen-terminated and oxidized silicon surfaces laid the groundwork to further pursue molecular modification of these classical semiconductor devices.

As the first attempt to create metal−molecule−silicon junctions, one can prepare organic thin films by either simple deposition or Langmuir−Blodgett technology.[5] Because these organic films are physically adsorbed on the silicon substrates (the film structure is hardly organized or closely packed),[14] a meaningful correlation between the molecular structure and device performance is difficult to define. With the emergence of self-assembly technique, organic monolayers have been grafted onto oxidized silicon surfaces by the reactions of organosilicon derivatives (e.g., alkylchlorosilanes, alkylalkoxysilanes, and alkylaminosilanes) with surface silanol groups.[14,15] Thereafter, silicon substrates modified with *n*-alkanesiloxane monolayers have been popularly used to fabricate metal−molecule−semiconductor junctions and their corresponding electrical characteristics extensively investigated.[6−8] Despite the excellent insulating properties of these organic monolayers,[6] as well as the intriguing electrical behavior at the interfaces,[8] the presence of a thin silicon oxide film in the junction is not favorable for electrical communication between the organic molecules and silicon substrates and for further miniaturization of the devices. Other efforts to fabricate molecularly controllable diode junctions on oxidized silicon (e.g., ionic interaction between the adsorbed molecule and surface) have been also demonstrated.[9]

One of the most promising advances in the covalent attachment of organic monolayers to semiconductor surfaces is the formation of robust organic monolayers on silicon via the Si−C bond,[16] which essentially opened a new avenue for the fabrication of oxide-free metal−molecule−silicon junctions. In contrast to the well-developed synthetic routes to alkyl monolayers on hydrogen-terminated silicon,[17] the understanding of the electrical properties of these "genuine" metal−molecule−silicon junctions

* To whom correspondence should be addressed. Fax: (604) 291-3765. E-mail: hzyu@sfu.ca.

10.1021/jp034791d CCC: $25.00
Published on Web 07/11/2003

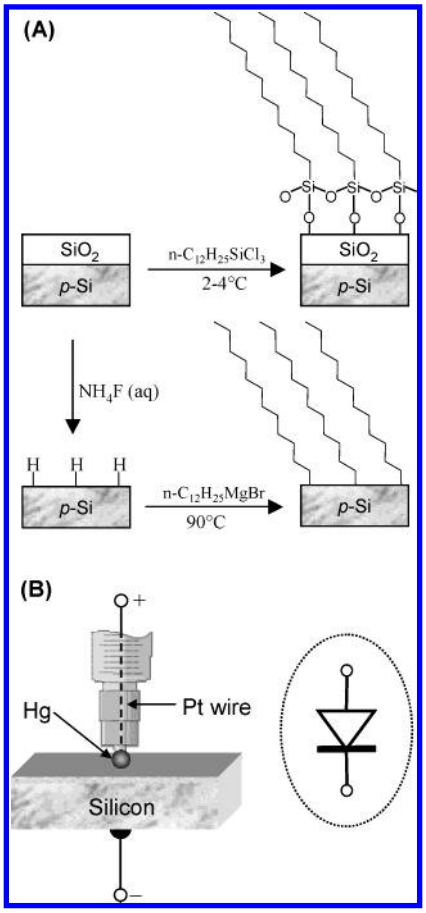

Figure 1. Schematic description of the modification routes (A) and the experimental setup (B) for the fabrication of diode junctions and electrical measurements.

is still very limited.[10] In addition to the studies of improved electrical properties of covalently linked polypyrrole|silicon junctions by Kim et al.[10a,b] and electrical characterization of Al|1-octadecyl monolayer|silicon junctions by Vuillaume and co-workers,[10c] we have reported the remarkable ideality and molecular tunability of mercury|alkyl monolayer|silicon (n-type) junctions recently.[10d,e]

The present report aims at a clear assessment of the correlation between electrical performance and passivation method (e.g., oxidation, alkylation, and alkylsilation) involved in the fabrication of modified mercury−silicon (p-type) junctions. Unlike *n*-type silicon reported previously,[10d,e] direct mercury−silicon (p-type) junctions exhibit near ideal diode behavior (as a result of the high barrier height),[4a−c] for which the contribution of organic monolayers and oxide thin films as electron (hole) tunneling barriers would not be as significant.[10d,e] Complementary to the recent studies of electron transport across metal−molecules−metal junctions,[18] this paper presents a comprehensive description of molecular passivation of interfaces and its impact on the electrical performance of the diode junctions (e.g., rectifying ratio, barrier height, and density of interface states). The potential of organic modification and the significance of surface engineering in the fabrication of novel silicon-based semiconductor devices have been demonstrated using model systems.

As a natural comparison, we have chosen *n*-dodecyl monolayers on silicon ($C_{12}H_{25}$−Si), oxidized silicon (SiO_2−Si), and *n*-dodecylsiloxane monolayers on oxidized silicon ($C_{12}H_{25}SiO_3$−SiO_2−Si) to fabricate diode junctions (Figure 1A). Both organic monolayers have similar thicknesses (which is also close to that of the oxide thin film) and similar packing properties, for which the impact of different monolayer structure on the electrical performance would be minimized. In addition, their preparation and characterization procedures have been well documented. In terms of device fabrication, mercury was used to form metal contacts on silicon surfaces (Figure 1B).[10d,e] This traditional approach,[19] was made popular recently by several research groups, because of the excellent surface property of mercury (atomically flat and capable of being modified with alkanethiolate monolayers) and also the ease in making reliable and reproducible measurements as demonstrated previously.[8c,d,10d,e,11a,18a,b]

2. Experimental Section

Silicon (111) wafers (p-type: 5−10 Ω·cm) were purchased from American Silicon Products, Inc.; *n*-dodecylmagnesium bromide in diethyl ether (1.0 M), *n*-dodecyltrichlorosilane (98%), and mercury (99.9999%) were purchased from Aldrich; trifluoroacetic acid (99.9%), tetrahydrofuran (THF), and *n*-dodecane (99.5%) were purchased from Caledon Laboratories Ltd. (Georgetown, ON); ammonium fluoride (40%) and sulfuric acid (96%) were purchased from GEM Microelectronic Materials (Chandler, AZ). All other chemicals were of ACS reagent grade and used as received without further purification.

2.1. Sample Preparation. *Oxidation.* Pieces of silicon wafers (1.5 × 2.0 cm^2) were initially cleaned in a "piranha" solution, i.e., 3:1 mixture of concentrated H_2SO_4 and H_2O_2 (30% aqueous solution) heated to 90 °C (CAUTION: *piranha" solution reacts violently with organic materials; it must be handled with extreme care*) for 30 min, followed by copious rinsing with deionized water. These cleaned silicon wafers, dried with ultrapure N_2, were used either for the preparation of Hg|SiO_2−Si junctions or for further modifications. To prepare hydrogen-terminated silicon (H−Si) sample (for the assembly of Hg|H−Si junctions and further modification with alkyl monolayers), the cleaned silicon wafers (covered with native silicon oxide films) were etched in deoxygenated NH_4F (40% aqueous) for 15 min. The samples were then transferred without rinsing into the reaction vessel for further derivatization. For comparison purposes, oxidized silicon substrates were also prepared by dipping fresh H−Si samples in "piranha" solution for 15 min.

Alkylation. *n*-Dodecyl monolayers on silicon were prepared as described in our previous work.[17e,20] The freshly etched H−Si sample was placed in a Schlenk tube containing 5 mL of deoxygenated *n*-dodecylmagnesium bromide (1.0 M solution in diethyl ether) and heated for 16−24 h in a constant-temperature bath set to 90 °C. Upon completion of the reaction, the modified silicon substrate was then rinsed with 1% CF_3-COOH solution in THF, Milli-Q water, and finally 1,1,1-trichloroethane before fabrication of the junctions.

Alkylsilation. The preparation of *n*-dodecylsiloxane monolayers on oxidized silicon was adapted from published procedures.[21] In brief, the oxidized silicon sample was dried in an oven at 100 °C at atmospheric pressure to remove the naturally adsorbed layer of water. Immediately after drying, the sample was immersed in a solution of 1.0 mM *n*-dodecyltrichlorosilane in 70% *n*-dodecane and 30% 1,1,1-trichloroethane and kept at 2−4 °C for 1 h. The silicon sample was then sonicated and rinsed for three times with 1,1,1-trichloroethane and dried using ultrapure N_2 before the fabrication of junctions.

2.2. Device Fabrication. Passivated mercury−silicon junctions were fabricated by making microcontacts on differently modified silicon surfaces. As shown in Figure 1B, a mercury drop extruded from a gastight syringe was brought into contact

TABLE 1: Surface and Structural Characterization of Differently Modified and Hydrogen-Terminated Silicon Surfaces

	contact angle/deg[22]		ellipsometric thickness/Å[23]
	H_2O	Hg	
SiO_2-Si	<5	122 ± 5	19.4 ± 1.5
$C_{12}H_{25}$–Si	103 ± 2	138 ± 2	14.2 ± 1.0
$C_{12}H_{25}SiO_3-SiO_2-Si$	112 ± 1	142 ± 3	16.2 ± 1.5
H−Si	90 ± 7	118 ± 5	N/A

with the silicon surface, and a platinum wire planted into the Teflon tip of the syringe plunger provided an electrical connection between the mercury and potentiostat. The approaching process was controlled by a custom-made micromanipulator and monitored by a video digital microscope with a 40× objective (model: DM143, Micro-Optic Industrial Group Co., Hong Kong). The contact area was measured accurately using the Motic Images 2000 Software provided by the manufacturer. The typical uncertainty of the measurements was ±20 μm for a junction with a 500 μm diameter, corresponding to a relative uncertainty of less than 10% in the actual contact area. The diameter of the contacts typically ranged from 400 to 600 μm (with a contact area of $1.2-2.8 \times 10^{-3}$ cm^2). Multiple junctions could be easily assembled on the same silicon sample by translating the silicon wafer to make new contacts on different areas.

2.3. Electrical Characterization. The electrical characterization was carried out using an Autolab Electrochemical Analyzer (model: PGSTAT30, Eco Chemie BV, The Netherlands) in a Faraday cage to prevent both room light illumination and electrical noise. For current density−bias voltage measurements ($J-V$), a linear scan was started from +0.5 V (forward bias, silicon as the anode) to −0.5 V (reverse bias, silicon as the cathode) with a step size of 0.007 V and a scan rate of 0.05 V/s. For differential capacitance−voltage ($C-V$) measurements, the choice of the scan range and frequency depended on the purpose of the experiments, as specified in the results sections. Repeated voltage scans did not show significant variation of the response, and no breakdown of the junctions was observed in either $J-V$ or $C-V$ measurements under typical experimental conditions.

3. Results

The surface and structural properties of the modified p-type silicon surfaces were thoroughly characterized by using wetting measurements, ellipsometry, and infrared (IR) spectroscopy.[22−25] As shown in Table 1, the wetting properties are quite different from the organic modified to oxidized samples in terms of the contact angles of water droplets. The hydrophobic nature of both $C_{12}H_{25}-Si$ and $C_{12}H_{25}SiO_3-SiO_2-Si$ surfaces indicates that these organic monolayers are closely packed. When mercury was used instead of water for the wetting measurements, the contact angles obtained were not very different from each other despite the different surface modifications. The ellipsometric thicknesses of the organic monolayers and the oxide thin films are close to each other, considering the uncertainties in the measurements (e.g., a value of the refractive index of the film must be assumed in order to determine the thickness of a film that is thinner than 50 Å).[23,25] Due to the presence of the Si−O−Si bonds, the thickness of a *n*-dodecylsiloxane monolayer is expected to be slightly larger than that of *n*-dodecyl monolayers. The organic monolayers are both, in fact, thinner than the native oxide films on silicon (p-type). As indicated by the band positions of the CH_2 asymmetric and symmetric stretch modes in their IR spectra (i.e., 2919.6 and 2850.7 cm^{-1} for $C_{12}H_{25}SiO_3-SiO_2-Si$; 2919.2 and 2849.3 cm^{-1} for $C_{12}H_{25}-Si$, figures not shown),[24] both monolayers are believed to be highly oriented at the molecular level.[14,15]

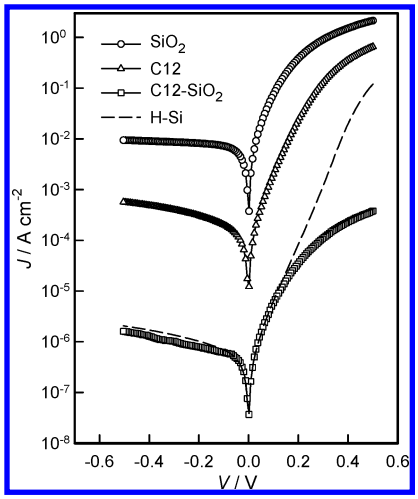

Figure 2. Representative current density−voltage ($J-V$) curves of junctions of Hg|SiO_2−Si, Hg|$C_{12}H_{25}$−Si, and Hg|$C_{12}H_{25}SiO_3-SiO_2$−Si (abbreviated as SiO_2, C12, and C12−SiO_2, respectively). A $J-V$ curve of Hg|H−Si (p-type) is shown for comparison (dashed line). Each curve is typical of at least 15 independent junctions.

3.1. Current−Voltage Properties. Figure 2 shows representative current densities of junctions Hg|SiO_2−Si, Hg|$C_{12}H_{25}$−Si, and Hg|$C_{12}H_{25}SiO_3-SiO_2$−Si as a function of applied bias voltage. For comparison, a typical current density−voltage curve of Hg|H−Si (p-type) is also shown as a dashed line. In contrast to the ohmic characteristics of Hg|H−Si (n-type),[10d] the direct Hg|H−Si (p-type) junctions behave as typical Schottky diodes.[4] Furthermore, all the passivated junctions exhibit clear rectifying behavior, i.e., the current at forward bias is significantly higher than the saturation current at reverse bias. We also noticed that for the modified junctions the saturation current densities at zero bias voltage showed considerable variations. In particular, the junction of Hg|SiO_2−Si has the highest current density while the Hg|$C_{12}H_{25}SiO_3-SiO_2$−Si displayed the lowest current density. In addition, the forward current density−voltage curves go downward at large applied voltages (>0.30 V) for junctions of Hg|SiO_2−Si and Hg|$C_{12}H_{25}SiO_3-SiO_2$−Si. From these current density−bias voltage curves (Figure 2), the rectifying ratios, effective barrier heights, and ideality factors can be evaluated, thus allowing us to quantify and compare the different electrical properties of the modified diode junctions.

Rectifying Ratio. Metal−semiconductor junctions have been widely used as rectifiers (e.g., Schottky diodes);[1] therefore, it is critical to compare the rectifying ratios of these molecularly modified junctions. The rectifying ratios (R_f) can be obtained by simply comparing the current density at forward bias with that at reverse bias, i.e., $R_f = |I(V)/I(-V)|$, which are plotted in Figure 3 for the passivated junctions. It is clear that there is no significant difference among these three different junctions at low applied voltage (<0.2 V). With increased applied bias, the rectifying ratio of Hg|$C_{12}H_{25}$−Si increases sharply while that of either Hg|SiO_2−Si or Hg|$C_{12}H_{25}SiO_3-SiO_2$−Si does not change as much. As a preliminary indication, this clearly demonstrates the more ideal diode characteristics of Hg|$C_{12}H_{25}$−Si compared to the mercury−silicon junctions passivated by either oxidation or alkylsilation.

Barrier Height, Ideality Factor, and Series Resistance. The fundamental parameter that describes electrical properties of a metal−semiconductor junction is the barrier height. According to the Mott−Schottky rule,[1a,b] for an ideal metal−semiconductor

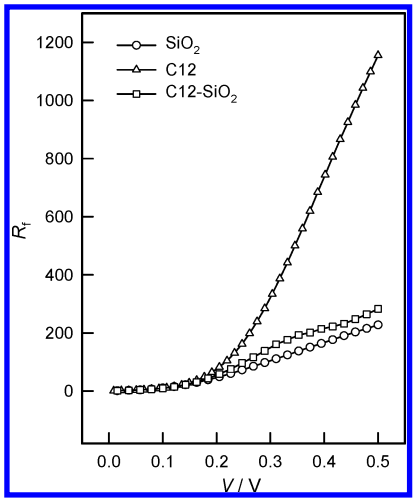

Figure 3. Rectifying ratio as a function of the applied voltage for junctions of Hg|SiO_2−Si (○), Hg|$C_{12}H_{25}$−Si (△), and Hg|$C_{12}H_{25}SiO_3$−SiO_2−Si (□).

(p-type) junction, the barrier height $q\phi_b$ is given by

$$q\phi_b = E_g - q(\phi_m - \chi_{sc}) \tag{1}$$

where $q\phi_m$ is the work function of the metal (the energy difference between the vacuum level and the Fermi level), $q\chi_{sc}$ is the electron affinity of the semiconductor measured from the bottom of the conduction band to the vacuum level, and E_g is band gap of the semiconductor. In practice, the effective barrier height,ϕ_{eff}, together with the ideality factor, n (a dimensionless parameter to take into account nonideal diode behaviors), were often determined from the analysis of the current density−voltage (J−V) characteristics using the classical thermionic emission theory[1a,b]

$$J = A^*T^2 \exp\left(-\frac{q\phi_{eff}}{kT}\right)\left(\frac{qV}{nkT} - 1\right) \tag{2}$$

where V is the applied bias voltage (in V), J is the measured current density (in A cm^{-2}), q is the absolute value of the electronic charge (in C), k and T are Boltzmann's constant and absolute temperature, respectively. A^* is the Richardson constant with a value of 32 A·cm^{-2}·K^{-2} for p-type silicon.[1c] A problem arises if it is necessary to extract reliable values of ϕ_{eff} when the diode has a large series resistance, R_s. It includes the metal resistance, ohmic contacts, and spreading resistance in the wafer. Equation 2 has been modified in order to model the effect of the series resistance, R_s, in the diode junctions,[26] particularly when the region over which the plot of ln J versus V is linear maybe small and accurate extrapolation to zero voltage may be difficult. In the case of $q(V - JR_s) > kT$[26a]

$$J = A^*T^2 \exp\left(-\frac{q\phi_{eff}}{kT}\right)\left(\frac{q(V - JR_s)}{nkT}\right) \tag{3}$$

Equation 3 can be rewritten as

$$V = JR_s + n\phi_{eff} + n\frac{kT}{q}\ln\left(\frac{J}{A^*T^2}\right) \tag{4}$$

Differentiating eq 4 with respect to J and rearranging terms, we obtain

$$\frac{dV}{d\ln J} = n\frac{kT}{q} + JR_s \tag{5}$$

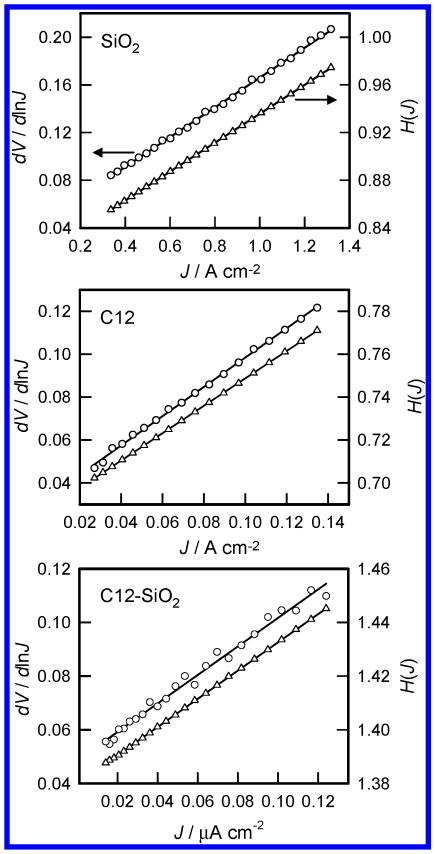

Figure 4. Plots of dV/(d ln J) vs J (○) and $H(J)$ vs J (△) for junctions of Hg|SiO_2−Si, Hg|$C_{12}H_{25}$−Si, and Hg|$C_{12}H_{25}SiO_3$−SiO_2−Si. Symbols are experimental data, and solid lines are the best least-squares fits to the linear region.

From eq 5, a plot of dV/(d ln J) vs J will give R_s as the slope and nkT/q as the y-axis intercept. To evaluate ϕ_{eff}, we can define a function $H(J)$

$$H(J) \equiv V - n\frac{kT}{q}\ln\left(\frac{J}{A^*T^2}\right) \tag{6}$$

From eq 4, we then have

$$H(J) = JR_s + n\phi_{eff} \tag{7}$$

According to eq 7, a plot of $H(J)$ vs J will also give a straight line with the y-axis intercept equal to $n\phi_{eff}$, from which the ϕ_{eff} can be derived by substituting in the n value obtained from eq 5. The slope of this plot also provides a second determination of R_s, which can be used to check the consistency of this approach.

We have applied the above procedure to examine the J−V characteristics of the passivated mercury−silicon junctions. As shown in Figure 4, both plots of dV/(d ln J) vs J and $H(J)$ vs J display linear behavior for all three types of junctions. The values R_s obtained from the two different plots agree well with each other within experimental uncertainties (determined from at least 15 independent junctions for each type). The evaluated diode parameters for both direct Hg|H−Si (p-type) and modified junctions are summarized in Table 2.

The obtained effective barrier height ($q\phi_{eff}$) of Hg|H−Si is consistent within experimental error to the value reported by Freeouf and Witter,[4a,b] particularly when we consider the difference in the preparation methods for H−Si surfaces. Furthermore, the effective barrier heights of the passivated junctions were surprisingly lower than that of Hg|H−Si, while

TABLE 2: Effective Barrier Height ($q\phi_{eff}$), Ideality Factor (n), and Series Resistance (R_s) of the Diode Junctions Extracted from the Current Density−Bias Voltage ($J-V$) Measurements

diode junctions	$q\phi_{eff}$/eV	n	$R_s/\Omega\cdot cm^{-2}$
Hg|SiO_2−Si	0.56 ± 0.07	1.43 ± 0.16	0.24 ± 0.10
Hg|$C_{12}H_{25}$−Si	0.66 ± 0.06	1.33 ± 0.10	0.50 ± 0.20
Hg|$C_{12}H_{25}SiO_3$−SiO_2−Si	0.76 ± 0.06	1.83 ± 0.18	560 ± 30
Hg|H−Si	0.83 ± 0.04	1.14 ± 0.08	N/A

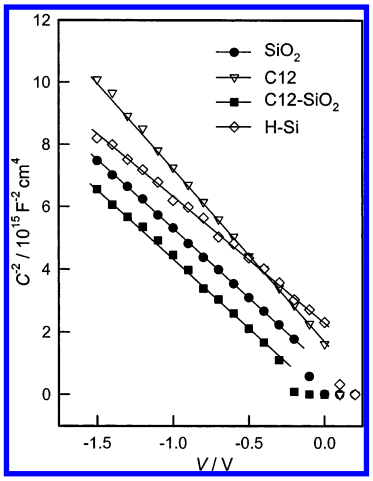

Figure 5. Representative C^{-2} vs V (Mott−Schottky) plots at the frequency of 1.0 MHz for junctions of Hg|SiO_2−Si (●), Hg|$C_{12}H_{25}$−Si (△), Hg|$C_{12}H_{25}$−SiO_2−Si (■), and Hg|H−Si (◇). The solid lines are the best linear fits to the experimental data. Each curve is typical of at least 15 independent junctions.

the deviation of ideality factors and the increase of series resistance are significant (see detailed discussion in section 4).

3.2. Capacitance−Voltage Properties. The overall differential capacitance of a metal−semiconductor contact is extremely sensitive to the interface properties.[1] This is particularly true with the presence of interfacial electronic states, which respond differently to low and high frequencies. To further examine the electrical properties and their correlation with interfacial characteristics of the passivated mercury−silicon junctions, differential capacitance−bias voltage ($C-V$) measurements were performed and analyzed.

Dopant Density and Surface Potential from Mott−Schottky Plots. For a metal−semiconductor contact with a thin interfacial insulator, the potential drops across the insulator are very small and the capacitance per unit area can be expressed under reversed bias[3a,27]

$$\frac{1}{C^2} = \frac{2(V_{d0} - V)}{q\epsilon_s\epsilon_0 N_d} \qquad (8)$$

where C is the capacitance per unit area, V the applied bias, V_{d0} the surface potential at zero bias, N_d the dopant density, ϵ_s the relative permittivity (dielectric constant) of the semiconductor, and ϵ_0 the permittivity of free space.

As shown in Figure 5, the Mott−Schottky plots ($C^{-2}-V$) are linear over a large bias voltage range (0 to −1.5 V) for both direct Hg|H−Si (p-type) and passivated junctions. It should be noted that the Mott−Schottky data were obtained at a high frequency (1.0 MHz). This is because at a low frequency the capacitance resulting from the interface states can follow the a.c. signal; therefore, the experimentally determined total capacitance equals to the sum of space−charge capacitance (C_{sc}) and the surface/interface state capacitance (C_{ss}). Only at high frequency, the total capacitance is approximately equal to the space−charge capacitance.[3a] According to eq 8, the dopant density (N_d) can be extracted from the slope and the surface potential V_{d0} can be obtained from the intercepts with the x-axis of the $C^{-2}-V$ plot (linear region). Table 3 summarizes the experimentally determined N_d and V_{d0} for the junctions studied.

TABLE 3: Differential Capacitance-Bias Voltage Properties of Molecularly Passivated Mercury−Silicon (p-type) Junctions[a]

	$N_d/10^{15}$ cm^{-3}	V_{d0}/V	$q\phi_b$/eV	$D_{it}/10^{12}$ eV^{-1} cm^{-2}
Hg|SiO_2−Si	2.7 ± 0.6	0.26 ± 0.06	0.50 ± 0.06	14[b]
Hg|$C_{10}H_{21}$−Si	2.1 ± 0.6	0.32 ± 0.08	0.56 ± 0.08	0.20[b]
Hg|$C_{12}H_{25}SiO_3$−SiO_2−Si	2.6 ± 0.6	0.09 ± 0.10	0.33 ± 0.10	0.12[c]
Hg|H−Si	3.0 ± 0.6	0.59 ± 0.05	0.82 ± 0.05	N/A

[a] The dopant density (N_d) and the surface potential (V_{d0}) were calculated from the fitting of Mott−Schottky plots (C^{2-} vs V). The dopant density calculated from the resistivity measurements was (2.1 ± 0.7) × 10^{15} cm^{-3}. [b] The density of interface states determined from eq 9 and at zero bias voltage. [c] It is not appropriate to compare this value directly with others, because of the irregular behavior of the capacitance as a function of the frequency for this particular system (see text for details).

It is clear that the dopant densities obtained from the best fits to the Mott−Schottky plots of both the direct Hg|H−Si and passivated junctions agree with the value (2.1 ± 0.7 × 10^{15} cm^{-3}) derived from the resistivity data within the experimental uncertainties. This indicates that neither organic modification nor oxidation changes the intrinsic properties of the silicon substrates and that there are no major orientation changes or defects in these organic monolayers on silicon under applied bias voltages. However, it should be also noticed that the surface potentials obtained for these diode junctions are clearly different from each other; in particular, values of V_{d0} for the passivated junctions shift significantly toward the negative with respect to Hg|H−Si.

Density Distribution of Interface States. The presence of interface states significantly alters the device performance of metal−semiconductor junctions, particularly the effective barrier height.[1] To give further insights into the electrical properties of these molecularly passivated mercury−silicon (p-type) junctions, we evaluated the density distribution of interface states from high- and low-frequency capacitance characteristics at forward bias based on a procedure previously reported.[5b,28]

Figure 6 shows the experimental high and low forward bias capacitance−voltage plot of the passivated mercury−silicon (p-type) diode junctions in the frequency range from 1.0 kHz to 1.0 MHz. The low-frequency capacitance increases with applied voltage (even goes through a maximum), while the high-frequency capacitance remains almost constant. The fact that a maximum is observed in the capacitance−voltage curves is clear evidence of the presence of series resistance in the diode junctions,[28a] which is consistent with the current density−voltage measurements described above (section 2.1). Differing from the typical features as mentioned above, the frequency dependence of the capacitance for the junctions of $C_{12}H_{25}SiO_3$−SiO_2−Si (bottom of Figure 6) does not follow a simple trend. Apart from a downward shift when the frequency becomes very high (1.0 MHz), no clear difference can be distinguished at lower frequencies (e.g., from 100 Hz to 100 kHz).

In classical metal−semiconductor devices with present interfacial thin films, interface states can be divided into two groups.[3a] In one group, the electronic states are in equilibrium

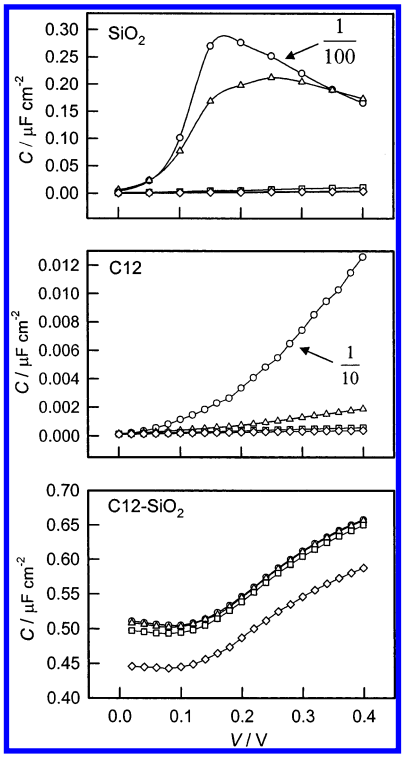

Figure 6. Representative capacitance−voltage ($C-V$) curves at the frequency of 1.0 K (○), 10 K (△), 100 K (□), and 1.0 MHz (◇) for junctions of Hg|SiO_2−Si, Hg|$C_{12}H_{25}$−Si, and Hg|$C_{12}H_{25}SiO_3$−SiO_2−Si, respectively. Each curve is typical of at least 15 independent junctions.

with the metal, while those of the other group are in equilibrium with the semiconductor. However, for junctions created from "soft" mercury contacts, it is reasonable to assume that all the interface states are in equilibrium with the semiconductor, i.e., they are located at the silicon/insulator interfaces. This is because mercury possesses an atomically flat surface, which is an excellent substrate to build metal−insulator−metal junctions (as shown by the contact angle measurements, see Table 1). In general, the interface states in equilibrium with the semiconductor do not contribute to the capacitance at high frequencies because the charges at the interface states cannot follow the fast a.c. signal as mentioned above. Therefore, the total capacitance determined experimentally is equal to the sum of space−charge capacitance (C_{sc}) and interface capacitance (C_{ss}) at low frequencies, while at high frequency the total capacitance arises mostly from the space−charge capacitance. By considering the difference between the low- and high-frequency values of the total capacitances, the interface states density (D_{it}) can be calculated by[28]

$$D_{it} = (q\epsilon_s\epsilon_0 N_d/2V_d)^{1/2}(C_{LF} - C_{HF})/qC_{HF} \quad (9)$$

where C_{LF} and C_{HF} are the low- and high-frequency capacitances, respectively. V_d is the surface potential at applied bias voltage (V) that can be calculated from[3a]

$$V_d = V_{d0} - \int_0^V \frac{1}{n}\,dV = V_{d0} - \frac{V}{n} \quad (10)$$

The interface state density D_{it} has been calculated from the experimental values of C_{LF} (1.0 kHz) and C_{HF} (1.0 MHz) using eq 9 as a function of applied bias voltage V. In a p-type semiconductor, the energy of the interface states, E_{ss} with respect to the top of the valance band (E_v) at the surfaces of the semiconductor is given by eq 11[5b,c]

$$E_{ss} - E_v = q\phi_b - qV \quad (11)$$

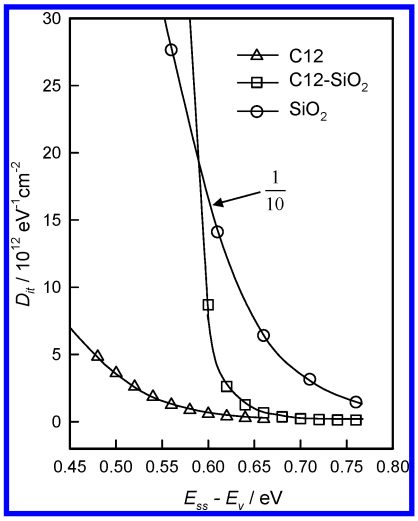

Figure 7. Energy distribution of interface state densities extracted from the low-frequency and high-frequency capacitance measurements for junctions of Hg|SiO_2−Si, Hg|$C_{12}H_{25}$−Si, and Hg|$C_{12}H_{25}SiO_3$−SiO_2−Si. The solid lines are only to guide the eyes.

With the help of eq 11, the D_{it} values as a function of the applied bias voltage V have been converted to a function of $E_{ss} - E_v$, and the energy distribution plot of the interfaces states (D_{it} vs $E_{ss} - E_v$) is shown in Figure 7.

As displayed in Figure 7, the general feature of the energy distribution curves of the interface states for the three types of passivated mercury−silicon junctions is similar, and it is consistent with those reported previously.[28] The interface state densities rise exponentially with bias voltage from the midgap toward the top of the valance band, while the absolute D_{it} values for differently passivated junctions showed significant variation. Apparently, the interface state densities for junctions of Hg|$C_{12}H_{25}$−Si and Hg|$C_{12}H_{25}SiO_3$−SiO_2−Si are two orders lower than that of Hg|SiO_2−Si. In addition, the interface state densities of Hg|$C_{12}H_{25}$−Si (Table 3) are close to the results of Al|$C_{18}H_{37}$−Si ($1.7-3.0 \times 10^{11}$ eV^{-1} cm^{-2}) determined differently.[10c]

4. Discussion

The experimental results described above demonstrate that the mercury−silicon (p-types) junctions passivated via oxidation, alkylation, or alkylsilation exhibit near-ideal diode characteristics, yet the differences in terms of their device performance are evident. This clearly indicates that the passivation with organic monolayers or oxide thin films does not alter the intrinsic properties of either the semiconductor itself or the metal−semiconductor junctions. It is more practically imperative yet remarkably interesting to note that organic modification showed privileged electrical performance compared to that of oxide thin films. At the same time, the alkyl monolayers formed on silicon showed improved rectifying behavior and lower density of interface states compared to alkylsiloxane monolayers on oxidized silicon. The following discussion aims to provide a "general" picture of the correlation between passivation route and electrical performance and a direct comparison to the junctions formed on n-type silicon surfaces.[10d,e]

Ideality Factor and Rectifying Ratio. We have shown previously that an alkyl monolayer can tune a resistor, i.e., a direct Hg|H−Si (n-type) contact, to a diode, i.e., a Hg|C_nH_{2n+1}−

Si (n-type) junction.[10d] In this case, the ideality factor, *n*, changed dramatically when the H−Si (n-type) was passivated with an alkyl monolayer (e.g., the *n* values of Hg|$C_{10}H_{21}$−Si junctions are very close to 1). For p-type silicon, the junctions modified with alkyl monolayers have a smaller *n* values compared with the junctions formed on either oxidized or alkylsilated samples, indicating that the diode performance of Hg|$C_{12}H_{25}$−Si junctions is more ideal than that of junctions formed either directly on oxidized silicon or after alkylsilation. We noted that the ideality factor of Hg|H−Si (p-type) junctions is smaller than that of molecularly modified junctions (such as Hg|$C_{12}H_{25}$−Si), which seemingly indicates that the passivation does not improve the diode characteristics of mercury|silicon (p-type) junctions. As an empirical parameter, the ideality factor is used to describe the deviation of current−voltage characteristics of a diode from the thermionic emission theory.[1a] A large ideality factor normally indicates that the diode is far from ideal (e.g., the junctions prepared on alkylsilated silicon surfaces). This is due to the presence of the thicker interfacial layer or to the recombination in the depletion region, and the current will not be solely determined by the thermionic emission theory. Nevertheless, the molecular passivation, particularly the modification of the silicon surface with alkyl monolayers, significantly improves the stability of the surface as well as the reproducibility of the measurements. For instance, when a hydrogen-terminated silicon (H−Si) surface is exposed to air under ambient conditions, the *J*−*V* properties of mercury−silicon junctions formed changed dramatically, because of both organic contamination and partial oxidation.[11]

The observed rectifying ratios, R_f, which compare the forward and reverse bias currents, are further indications that the mercury−silicon junctions passivated via alkylation are better diodes than those prepared via either oxidation or alkylsilation. The nonlinear behavior of ln *J* vs *V* at higher applied voltage (Figure 2), particularly near the limiting current densities (where application of the classical thermionic model is not appropriate),[1a] dominates the variation of rectifying ratio as a function of applied bias voltage. As shown in Figure 2, the semilog *J*−*V* curve of Hg|$C_{12}H_{25}$−Si shows a much wider linear range, while those of Hg|SiO_2−Si and Hg|$C_{12}H_{25}SiO_3$−SiO_2−Si approach their limit currents at much lower bias voltage. The series resistance should be considered as one of the important factors, particularly in the case of Hg|$C_{12}H_{25}SiO_3$−SiO_2−Si (the large R_s value will make a significant noncompensate contribution to the voltage drop, JR_S). In the case of Hg|SiO_2−Si, although the absolute value of R_s is relatively small, the contribution of JR_S is still substantial because of the high current density, which is a result of the low barrier height (Table 2).

Effective Barrier Height and Surface Potentials. The effective barrier heights (ϕ_{eff}) for the direct Hg|H−Si (p-type) and passivated junctions derived from Figure 2 with the help of the Cheung's plots (eqs 6 and 7) are also very different from each other. In particular, the barrier heights of the modified junctions are lower than that of direct Hg|H−Si junctions, which is seemingly in contradiction with the expected contributions of the interfacial layer to the effective barrier height (ϕ_{eff}).[10d,e] This also reminds us of the discrepancy between the surface potentials at zero bias, V_{d0}, obtained from the Mott−Schottky (C^{-2} vs *V*) measurements for the direct and modified mercury−silicon junctions (Table 3), because the barrier height (ϕ_b) is correlated with the surface potential V_{d0} by[1c,3a]

$$\phi_b = V_{d0} + V_n = V_{d0} + \frac{kT}{q}\ln\frac{N_c}{N_d} \qquad (12)$$

in which V_n is the energy difference between the Fermi level and the valence band in the bulk and N_c is the carrier density in the conduction band of the semiconductor, N_c (Si) = 2.78 × 10^{19} cm^{-3}.[1c]

The surface potential is the barrier height seen by electrons (n-type semiconductor) or holes (p-type semiconductor) moving from semiconductor into metal. If the work function (ϕ_m) of the metal is lower than that of the semiconductor (ϕ_s), the surface potential (V_{d0}) at zero bias of an ideal metal−semiconductor (p-type) junction can be calculated by

$$qV_{d0} = q\phi_s - q\phi_m \qquad (13)$$

For an ideal mercury−silicon (p-type), The qV_{d0} value calculated from eq 13 should equal to 0.39 eV,[28] a value that deviates from the experimentally determined qV_{d0} values. As shown in Table 3, the V_{d0} value experimentally determined for Hg|H−Si is more positive than the theoretical one. At the same time, the surface potentials at zero bias voltage (qV_{d0}) of the passivated junctions are more negative than that of Hg|H−Si. In particular, the Mott−Schottky curves corresponding to the junctions formed on alkylsilated silicon exhibited the largest negative shift (see Figure 5).

In retrospect, the fixed charges in the insulator layers have been considered as the origin of the surface potential shifts with respect to the theoretical value in nonideal metal−semiconductor devices.[1b] For the junctions formed on oxidized silicon, it has been proposed that fixed charges inevitably located at the Si−SiO_2 interface arise mainly from the excess of silicon (trivalent) or from the loss of an electron from excess oxygen centers (nonbridging oxygen).[1b,3e] These fixed charges are, in general, positive and depend on the preparation of the oxide thin films and the intrinsic properties of silicon substrates. In the Mott−Schottky measurements, positive charges will induce a negative shift to the C^{-2}−*V* curves while negative ones will shift the C^{-2}−*V* curves positively.[1b] Because of the less polar nature of the alkyl monolayers formed on atomically flat H−Si (111) via Si−C bonding, the fixed charge density would be much lower than that of the thin oxide films. In contrast, the alkylsiloxane monolayers on oxidized silicon would have a much higher density of fixed charges because of the presence of two interfaces (i.e., SiO_2−Si and R−SiO_3−SiO_2). The positive shift of the surface potential for Hg|H−Si junctions might be due to the presence of fixed negative charges at the hydrogen layer−bulk silicon interface, for which further detailed studies are deserved.

To eliminate the influence of fixed charges in the insulating films on the surface potentials (and therefore the effective barrier heights), we normalized the *J*−*V* curves shown in Figure 2 to a common V_{d0} value of 0.39 eV. This was accomplished by introducing a factor, $\exp[-(q/kT)(V_{d0} - 0.39)]$, into eq 2 for the current density.[3a] The normalized semilog current density−bias voltage curves of the direct and passivated junctions formed on p-type silicon surfaces and the recalculated effective barrier heights (i.e., after normalization) are shown in Figure 8.

Comparing this with Figure 2, the *J*−*V* curves of the modified junctions are all shifted below that of Hg|H−Si junction. The effective barrier heights for these passivated junctions after normalization are also very different from those listed in Table 2. As described in eq 1, for an ideal metal−semiconductor (p-type) junction, the barrier height $q\phi_b$ is determined by the metal work function ($q\phi_m$), the semiconductor electron affinity (χ_{sc}), and the band gap of the semiconductor (E_g).[1] The barrier height determined in this fashion for Hg|H−Si (p-type) junctions would

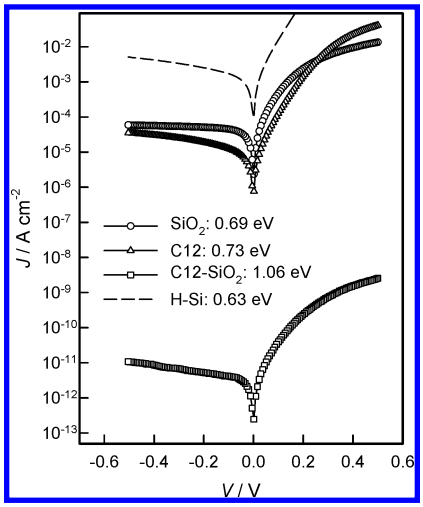

Figure 8. Current density−bias voltage ((*J*−*V*) curves of junctions of Hg|SiO_2−Si, Hg|$C_{12}H_{25}$−Si, and Hg|$C_{12}H_{25}SiO_3$−SiO_2−Si and the corresponding effective barrier height after normalization by a factor of exp[−(*q*/*kT*)(V_{d0} − 0.39)]. The normalized *J*−*V* curve of Hg|H−Si is also shown for comparison (dashed line).

be 0.64 eV, which is in excellent agreement with our measurements (0.63 ± 0.04 eV).

In the case where the metal is separated from the semiconductor by an ultrathin insulating film, the effective barrier height ($q\phi_{eff}$) can be evaluated as[8d,10d]

$$q\phi_{eff} = q\phi_b + kT\beta l \qquad (14)$$

The term of $kT\beta l$ describes the contribution to the effective barrier height of the interfacial layer, where β is the structure-dependent attenuation factor that depends on the charge transport mechanism[8c,d,10d,e,18,30] and *l* is the thickness of the insulating films. According to eq 14, we see that at least two factors directly affect the effective barrier height. As mentioned above, $q\phi_b$ is the barrier height presented to the electrons by the metal−semiconductor interface alone (which should be identical for all the three types of modified mercury−silicon junctions but is influenced by the density of interfacial states as discussed below). The other is the effect of the insulating layer that serves as a barrier to charge transport (tunneling) across the junction.

It is easy to understand that the junctions formed on alkylsilated silicon possess the highest effective barrier height because of the presence of both the oxide film and the organic monolayer. The excellent insulating properties of these monolayers have been confirmed by Vuillaume and co-workers.[6] Practically, contributions of the interfacial insulating layers can be estimated by using the $kT\beta l$ term in eq 14. Using the β value of 0.65 Å^{-1} for holes transfer through all-trans alkyl chains,[8d] the predicted increase of effective barrier height for Hg|$C_{12}H_{25}$−Si is 0.24 eV; for Hg|SiO_2−Si, using the results reported by Card et al. (taking βl as 7.1),[3a] it will be 0.18 eV. Similarly, the increase of barrier height for junction Hg|$C_{12}H_{25}SiO_3$−SiO_2−Si is 0.45 eV. In fact, this comparison provides a semiquantitative understanding of the difference between the normalized barrier heights of these passivated junctions as listed in Figure 8.

The comparison between the densities of the surface states in these molecularly modified mercury−silicon junctions also helps us to further understand the difference in the determined effective barrier heights (Table 2). Although all these junctions were fabricated from the same metal and semiconductor, in a real diode the barrier height ϕ_b is also greatly affected by the density of the surface states and the interfacial insulating layer (beyond the contribution as an electron tunneling barrier as discussed previously).[1,10e] The overall effect is that the lower the surface states density, the higher the barrier height is,[10d,e] which contributes to the fact that the effective barrier height of Hg|$C_{12}H_{25}$−Si (p-type) is higher than that of Hg|SiO_2−Si junctions, as shown in Table 2. The Hg|$C_{12}H_{25}SiO_3$−SiO_2−Si system is more complex due to the presence of two interfaces, for which the determination and comparison of its interface state density with other systems are difficult.

5. Conclusions

In summary, the electrical performance of the molecularly passivated metal−semiconductor junctions is dominated by the modification method and corresponding interfacial properties. In particular, the direct comparison between the mercury−silicon (p-type) junctions formed on alkylated, oxidized, or alkylsilated samples showed a clear correlation between the electrical property and the passivation route. As demonstrated experimentally, *n*-dodecyl monolayer modified mercury−silicon junctions display better rectifying behavior, i.e., larger rectifying ratio and smaller ideal ideality factor (close to unity), than those passivated with SiO_2 thin films and *n*-dodecylsiloxane monolayers (formed on oxidized silicon). The differential capacitance measurements indicated the presence of a large amount of positive charges in the oxide film and alkylsiloxane monolayer modified junctions. In addition, the organic modified junctions (both alkylation and alkylsilation) were confirmed to have substantially lower densities of surface states in comparison with that of Hg|SiO_2−Si. It may be premature to propose immediate applications of organic modified metal−semiconductor junctions, but continued research efforts in this field are warranted in order to probe the feasibility of introducing molecular engineering into silicon-based microelectronic devices.

Acknowledgment. The authors are grateful to the Natural Science and Engineering Research Council of Canada (NSERC) and Simon Fraser University for financial support. We wish to thank Dr. Steven A. Mitchell (NRC Canada) for his help with ellipsometry measurements.

References and Notes

(1) (a) Rhoderich, E. H.; Williams, R. H. *Metal-Semiconductor Contacts*, 2nd ed.; Clarendon Press: Oxford, 1988. (b) Sze, S. M. *Physics of Semiconductor Devices*, 2nd ed.; John Wiley & Sons: New York, 1981. (c) Singh, J. *Semiconductor Devices, Basic Principles*; John Wiley & Sons: New York, 2001.

(2) For examples of recent reviews, see: (a) Ashkenasy, G.; Cahen, D.; Cohen, R.; Shanzer, A.; Vilan, A. *Acc. Chem. Res.* **2002**, *35*, 121. (b) Carroll, R. L.; Gorman, C. B. *Angew. Chem., Int. Ed.* **2002**, *41*, 4378. (c) Cahen, D.; Kahn, A. *Adv. Mater.* **2003**, *15*, 271.

(3) (a) Card, H. C.; Rhoderich, E. H. *J. Phys. D: Appl. Phys.* **1971**, *4*, 1589. (b) Walker, L. G. *Solid-State Electron.* **1974**, *17*, 763. (c) Chattopadhyay, P.; Daw, A. N. *Solid-State Electron.* **1986**, *29*, 555. (d) Türüt, A.; Yalçin, N.; Sağlam, M. *Solid-State Electron.* **1992**, *35*, 835. (e) Wang, Q.; Liu, D.; Virgo, J. T.; Yeh, J.; Hillard, R. J. *J. Vac. Sci. Technol. A* **2000**, *18*, 1308. (f) Temircl, C.; Bati, B.; Sağlam, M.; Türüt, A. *Appl. Surf. Sci.* **2001**, *172*, 1. (g) Selzer, Y.; Cahen, D. *Adv. Mater.* **2001**, *13*, 508. (g) Asuha, Kobayashi, T.; Maida, O.; Inoue, M.; Takahashi, M.; Todokoro, Y.; Kobayashi, H. *Appl. Phys. Lett.* **2002**, *81*, 3410.

(4) (a) Wittmer, M.; Freeouf, J. L. *Phys. Lett. A* **1993**, *173*, 190. (b) Wittmer, M.; Freeouf, J. L. *Phys. Rev. Lett.* **1992**, *69*, 2701. (c) Kampen, T. U.; Monch, W. *Surf. Sci.* **1995**, *331*, 490. (d) Grupp, C.; Taleb-Ibrahimi, A. *Surf. Sci.* **1999**, *433*, 585.

(5) (a) Kaneko, F.; Shibata, M.; Inaba, Y.; Kobayashi, S. *Thin Solid Films* **1989**, *179*, 121. (b) Cakar, M.; Temirci, C.; Türüt, A. *ChemPhysChem.* **2002**, *3*, 701. (c) Cakar, M.; Onganer, Y.; Türüt, A. *Synth. Met.* **2002**, *126*, 213.

(6) (a) Fontaine, P.; Goguenheim, D.; Deresmes, D.; Vuillaume, D. *Appl. Phys. Lett.* **1993**, *62*, 2256. (b) Boulas, C.; Davidovits, J. V.; Rondelez, F.; Vuillaume, D. *Phys. Rev. Lett.* **1996**, *76*, 4797. (c) Vuillaume, D.; Boulas,

C.; Collet, J.; Davidovits, J. V.; Rondelez, F. *Appl. Phys. Lett.* **1996**, *69*, 1646. (d) Collet, J.; Lenfant, S.; Vuillaume, D.; Bouloussa, O.; Rondelez, F.; Gay, J. M.; Kham, K.; Chevrot, C. *Appl. Phys. Lett.* **2000**, *76*, 1339.

(7) Krishnamoorthy, A.; Chanda, K.; Murarka, S. P.; Ramanath, G.; Ryan, J. G. *Appl. Phys. Lett.* **2001**, *78*, 2467.

(8) (a) Cohen, R.; Zenou, N.; Cahen, D.; Yitzchaik. S. *Chem. Phys. Lett.* **1997**, *279*, 270. (b) Chai, L.; Cahen, D. *Mater. Sci. Eng. C* **2002**, *19*, 339. (c) Selzer, Y.; Salomon, A.; Cahen, D. *J. Am. Chem. Soc.* **2002**, *124*, 2886. (d) Selzer, Y.; Salomon, A.; Cahen, D. *J. Phys. Chem. B* **2002**, *106*, 10432.

(9) Li, D. Q.; Bishop, A.; Gim, Y.; Shi, X. B.; Fitzsimmons, M. R.; Jia, Q. X. *Appl. Phys. Lett.* **1998**, *73*, 2645.

(10) (a) Kim, N. Y.; Laibinis, P. E. *J. Am. Chem. Soc.* **1999**, *121*, 7162. (b) Vermeir, I. E.; Kim, N. Y.; Laibinis, P. E. *Appl. Phys. Lett.* **1999**, *74*, 3860. (c) Kar, S.; Miramond, C.; Vuillaume, D. *Appl. Phys. Lett.* **2001**, *78*, 1288. (d) Liu, Y. J.; Yu, H. Z. *ChemPhysChem* **2002**, *3*, 799. (e) Liu, Y. J.; Yu, H. Z. *ChemPhysChem* **2003**, *4*, 335.

(11) (a) Licciardello, A.; Puglisi, O.; Pignataro, S. *Appl. Phys. Lett.* **1986**, *48*, 41. (b) Miura, T.; Niwano, M.; Shoji, D.; Miyamoto, N. *J. Appl. Phys.* **1996**, *79*, 4373. (c) Ye, S.; Ichihara, T.; Uosaki, K. *Appl. Phys. Lett.* **1999**, *75*, 1562. (d) Liu, Y. J.; Waugh, D. M.; Yu, H. Z. *Appl. Phys. Lett.* **2002**, *81*, 4967.

(12) Dabrowski, J.; Mussig, H.-J. *Silicon Surfaces and Formation of Interfaces: Basic Science and the Industrial World*; World Scientific Publishing Co.: Singapore, 2000.

(13) (a) International Technology Roadmap for Semiconductors, Homepage, 2003, http://public.itrs.net. (b) Muller, D. A.; Sorsch, T.; Moccio, S.; Baumann, F. H.; Evans-Lutterodt, K.; Timp, G. *Nature* **1999**, *399*, 758.

(14) Ulman, A. *An Introduction to Ultrathin Organic Films: From Langmuir−Blodgett to Self-Assembly*; Academic Press: New York, 1991.

(15) Ulman, A. *Chem. Rev.* **1996**, *96*, 1533.

(16) For recent reviews, see: (a) Sieval, A. B.; Linke, R.; Zuihof, H.; Sudhölter, E. J. R. *Adv. Mater.* **2000**, *12*, 1457. (b) Wayner, D. D. M.; Wolkow, R. A. *J. Chem. Soc., Perkin Trans. 2* **2002**, 23. (c) Buriak, J. M. *Chem. Rev.* **2002**, *102*, 1271.

(17) (a) Linford, M. R.; Fenter, P.; Eisenberger, P. M.; Chidsey, C. E. D. *J. Am. Chem. Soc.* **1995**, *117*, 3145. (b) Bansal, A.; Li, X.; Lauermann, I.; Lewis, N. S.; Yi, S. I.; Weinberg, W. H. *J. Am. Chem. Soc.* **1996**, *118*, 7225. (c) Villeneuve, C. H.; Pinson, J.; Bernard, M. C.; Allongue, P. *J. Phys. Chem. B* **1997**, *101*, 2415. (d) Sieval, A. B.; Vleeming, V.; Zuilhof, H.; Sudhölter, E. J. R. *Langmuir* **1999**, *15*, 8288. (e) Boukherroub, R.; Morin, S.; Bensebaa, F.; Wayner, D. D. M. *Langmuir* **1999**, *15*, 3831.

(18) For examples, see: (a) Slowinski, K.; Fong, H. K. Y.; Majda, M. *J. Am. Chem. Soc.* **1999**, *121*, 7257. (b) Holmin, R. E.; Haag, R.; Ismagilov, R. F.; Mujica, V.; Ratner, M. A.; Rampi, M. A.; Whitesides, G. M. *Angew. Chem., Int. Ed.* **2001**, *40*, 2316. (c) Fan, F.-R. F.; Yang, J.; Dirk, S.; Price, D. W.; Kosynkin, D.; Tour, J. M.; Bard, A. J. *J. Am. Chem. Soc.* **2001**, *123*, 2454. (d) Wold, D. J.; Frisbie, C. D. *J. Am. Chem. Soc.* **2001**, *123*, 5549. (e) Leatherman, G.; Durantini, E. N.; Gust, D.; Moore, T. A.; Stone, S.; Zhou, Z.; Rez, P.; Liu, Y. Z.; Lindsay, S. M. *J. Phys. Chem. B* **1999**, *103*, 4006.

(19) (a) Mann, B.; Kuhn, H. *J. Appl. Phys.* **1971**, *42*, 4398. (b) Honig, E. P. *Thin Solid Films* **1976**, *33*, 231.

(20) (a) Yu, H. Z.; Morin, S.; Wayner, D. D. M.; Allongue, P.; Henry de Villeneuve, C. *J. Phys. Chem. B* **2000**, *104*, 11157. (b) Yu, H. Z.; Boukherroub, R.; Morin, S.; Wayner, D. D. M. *Electrochem. Commun.* **2000**, *2*, 562.

(21) (a) Brzoska, J. B.; Ben Azouz, I.; Rondelez, F. *Langmuir* **1994**, *10*, 4367. (b) Parikh, A. N.; Allara, D. L.; Parikh, A. N.; Rondelez, F. *J. Phys. Chem.* **1994**, *98*, 7577.

(22) The contact angles provided here are thermodynamic equilibrated contact angles of sessile liquid drops, which are believed to be smaller than advancing contact angles. They were determined on an AST Optima contact angle system at ambient conditions (18−22 °C, 30−35% relative humidity).

(23) Ellipsometric measurements were performed with a Gaertner variable angle ellipsometer L116B using a helium−neon laser at an incident angle of 70°. The monolayer thickness was calculated using an index of refraction of 1.46 for both the hydrocarbon monolayers and silicon oxide.

(24) The attenuated total reflection−absorption (ATR) infrared spectra were recorded using a Nicolet Nexus-IR 560 spectrometer at a 0.5 cm^{-1} resolution. The ATR crystals ($25 \times 5 \times 1$ mm^3) were mounted in a purged sample chamber with the light focused normal to one of the 45° bevels. Background spectra were obtained using a freshly prepared oxidized silicon surface.

(25) Wasserman, S. R.; Whitesides, G. M.; Tidswell, I. M.; Ocko, B. M.; Pershan, P. S.; Axe, J. D. *J. Am. Chem. Soc.* **1989**, *111*, 5852.

(26) (a) Cheung, S. K.; Cheung, N. W. *Appl. Phys. Lett.* **1986**, *49*, 85. (b) Werner, J. H. *Appl. Phys. A* **1988**, *47*, 291. (c) Ayyildiz, E.; Türüt, A.; Efeoğlu, H.; Tüzemen, S.; Sağlam, M.; Yoğurtçu, Y. K. *Solid-State Electron.* **1996**, *39*, 83.

(27) Sharma, B. L. *Metal-Semiconductor Schottky Barrier Junctions and Their Applications*; Plenum Press: New York, 1984.

(28) (a) Chattopadhyay, P.; RayChaudhuri, B. *Solid-State Electron.* **1993**, *36*, 605. (b) Chattopadhyay, P. *Solid-State Electron.* **1996**, *39*, 1491. (c) Pandey, S.; Kal, S. *Solid-State Electron.* **1998**, *42*, 943.

(29) For p-type semiconductor, the work function ($q\phi_s$) can be derived from $q\phi_s = q\chi_{sc} + E_g - V_n$. The calculated $q\phi_s$ is 4.88 eV for p-type silicon with a dopant density of 2.1×10^{15} cm^{-3}; for mercury the $q\phi_m$ is 4.49 eV (see, Michaelson, H. B. *J. Appl. Phys.* **1977**, *48*, 4729).

(30) According to ref 3f (*Appl. Surf. Sci.* **2001**, *172*, 1−7), the quantity of βl can be further evaluated as the hole-tunneling factor, $a\delta(\chi)^{1/2}$, where $a = (4\pi/h)(2m^*)^{1/2}$ is a constant dependent on effective mass, $m^* = 0.16m_0$ is the effective barrier tunneling mass of holes, χ is the effective barrier height presented by the thin interfacial layer, and δ is the thickness of the interfacial layer.